

Beyond the “faster is slower” effect

I.M. Sticco and F.E. Cornes

*Departamento de Física, Facultad de Ciencias Exactas y Naturales, Universidad de Buenos Aires,
Pabellón I, Ciudad Universitaria, 1428 Buenos Aires, Argentina.*

G.A. Frank

*Unidad de Investigación y Desarrollo de las Ingenierías,
Universidad Tecnológica Nacional, Facultad Regional Buenos Aires,
Av. Medrano 951, 1179 Buenos Aires, Argentina.*

C.O. Dorso*

*Departamento de Física, Facultad de Ciencias Exactas y Naturales, Universidad de Buenos Aires,
Pabellón I, Ciudad Universitaria, 1428 Buenos Aires, Argentina. and
Instituto de Física de Buenos Aires, Pabellón I,
Ciudad Universitaria, 1428 Buenos Aires, Argentina.*

(Dated: October 13, 2018)

The “faster is slower” effect raises when crowded people push each other to escape through an exit during an emergency situation. As individuals push harder, a statistical slowing down in the evacuation time can be achieved. The slowing down is caused by the presence of small groups of pedestrians (say, a small human cluster) that temporarily blocks the way out when trying to leave the room. The pressure on the pedestrians belonging to this blocking cluster raises for increasing anxiety levels and/or larger number of individuals trying to leave the room through the same door. Our investigation shows, however, that very high pressures alters the dynamics in the blocking cluster, and thus, changes the statistics of the time delays along the escaping process. It can be acknowledged a reduction in the long lasting delays, while the overall evacuation performance improves. We present results on this novel phenomenon taking place beyond the “faster is slower” regime.

PACS numbers: 45.70.Vn, 89.65.Lm

I. INTRODUCTION

The “faster is slower” (FIS) effect is the major phenomenon taking place when pedestrians get involved in a dangerous situation and try to escape through an emergency door. It states that the faster they try to reach the exit, the slower they move due to clogging near the door. This effect has been observed in the context of the “social force model” (SFM) [1]. But research on other physical systems, such as grains flowing out a 2D hopper or sheep entering a barn, are also known to exhibit a “faster is slower” behavior [2].

Research on the clogging delays (in the context of the SFM) has shown that a small group of pedestrians close to the door is responsible for blocking the way to the rest of the crowd. This *blocking clusters* appear as an arch-like metastable structure around the exit. The tangential friction between pedestrians belonging to this blocking structure was shown to play a relevant role with respect to the whole evacuation delays [3, 4]. However, either the amount of blocking structures or its time life can vary according to the door width, the presence of obstacles or fallen individuals [5, 6]. Further

studies on blocking structures appearing in granular media research can be found in Refs. [7–10].

The relevance of the *blocking structures* on the time evacuation performance has alerted researchers that the analysis of “reduced” systems rather than the whole crowd is still a meaningful approach to the FIS effect. In this context, the authors of Ref. [11] introduced a simplified breakup model for a small arch-like blocking structure (in a SFM setting). They examined theoretically the breakup of the arch due to a single moving particle, and observed a FIS-like behavior. Thus, they concluded that the essentials of the FIS phenomenon could be described with a system of only a few degrees of freedom.

To our knowledge, neither the theoretical approach nor the computational simulations have been pushed to extreme scenarios. That is, no special attention has been paid to those situations where the pedestrians experience very high anxiety levels (see Section IV) while the crowd becomes increasingly large.

In the current investigation we explore the pedestrians anxiety levels from a relaxed situation to desired velocities that may cause dangerous pressures. A dangerous pressure of 1600 Nm^{-1} may be associated to at least three pedestrians pushing with a desired velocity close

* codorso@df.uba.ar

to 20 m/s (see Refs. [1, 12]).

Our work is organized as follows: a brief review of the basic SFM can be found in Section II. Section III details the simulation procedures used to studying the room evacuation of a crowd under panic. The corresponding results are presented in Section IV. Finally, the conclusions are summarized in Section V.

II. BACKGROUND

A. The Social Force Model

Our research was carried out in the context of the “social force model” (SFM) proposed by Helbing and co-workers [1]. This model states that human motion is caused by the desire of people to reach a certain destination, as well as other environmental factors. The pedestrians behavioral pattern in a crowded environment can be modeled by three kind of forces: the “desire force”, the “social force” and the “granular force”.

The “desire force” represents the pedestrian’s own desire to reach a specific target position at a desired velocity v_d . But, in order to reach the desired target, he (she) needs to accelerate (decelerate) from his (her) current velocity $\mathbf{v}^{(i)}(t)$. This acceleration (or deceleration) represents a “desire force” since it is motivated by his (her) own willingness. The corresponding expression for this forces is

$$\mathbf{f}_d^{(i)}(t) = m_i \frac{v_d^{(i)} \mathbf{e}_d^{(i)}(t) - \mathbf{v}^{(i)}(t)}{\tau} \quad (1)$$

where m_i is the mass of the pedestrian i . \mathbf{e}_d corresponds to the unit vector pointing to the target position and τ is a constant related to the relaxation time needed to reach his (her) desired velocity. Its value is determined experimentally. For simplicity, we assume that v_d remains constant during an evacuation process and is the same for all individuals, but \mathbf{e}_d changes according to the current position of the pedestrian. Detailed values for m_i and τ can be found in Refs. [1, 5].

The “social force” represents the psychological tendency of two pedestrians, say i and j , to stay away from each other by a repulsive interaction force

$$\mathbf{f}_s^{(ij)} = A_i e^{(r_{ij}-d_{ij})/B_i} \mathbf{n}_{ij} \quad (2)$$

where (ij) means any pedestrian-pedestrian pair, or pedestrian-wall pair. A_i and B_i are fixed values, d_{ij} is the distance between the center of mass of the pedestrians i and j and the distance $r_{ij} = r_i + r_j$ is the sum of the pedestrians radius. \mathbf{n}_{ij} means the unit vector in the

$\vec{j}i$ direction.

Any two pedestrians touch each other if their distance d_{ij} is smaller than r_{ij} . In this case, an additional force is included in the model, called the “granular force”. This force is considered be a linear function of the relative (tangential) velocities of the contacting individuals. Its mathematical expression reads

$$\mathbf{f}_g^{(ij)} = \kappa (r_{ij} - d_{ij}) \Theta(r_{ij} - d_{ij}) \Delta \mathbf{v}^{(ij)} \cdot \mathbf{t}_{ij} \quad (3)$$

where κ is a fixed parameter. The function $\Theta(r_{ij} - d_{ij})$ is zero when its argument is negative (that is, $r_{ij} < d_{ij}$) and equals unity for any other case (Heaviside function). $\Delta \mathbf{v}^{(ij)} \cdot \mathbf{t}_{ij}$ represents the difference between the tangential velocities of the sliding bodies (or between the individual and the walls).

The above forces actuate on the pedestrians dynamics by changing his (her) current velocity. The equation of motion for pedestrian i reads

$$m_i \frac{d\mathbf{v}^{(i)}}{dt} = \mathbf{f}_d^{(i)} + \sum_{j=1}^N \mathbf{f}_s^{(ij)} + \sum_{j=1}^N \mathbf{f}_g^{(ij)} \quad (4)$$

where the subscript j represents all the other pedestrians (excluding i) and the walls.

B. Clustering structures

The time delays during an evacuation process are related to clogged people, as explained in Refs. [3, 4]. Groups of pedestrians can be defined as the set of individuals that for any member of the group (say, i) there exist at least another member belonging to the same group (j) in contact with the former. That is, the distance between them (d_{ij}) is less than the sum of their radius ($d_{ij} < r_i + r_j$). This kind of structure is called a *human cluster* and it can be mathematically defined as

$$i \in \mathcal{G} \Leftrightarrow \exists j \in \mathcal{G} / d_{ij} < r_i + r_j \quad (5)$$

where \mathcal{G} corresponds to any set of individuals.

During an evacuation process, different human clusters may appear inside the room. But, some of them are able to *block* the way out. We are interested in the minimum set of human clusters that connects both sides of the exit. Thus, we will call *blocking clusters* or *blocking structures* to those human structures that block the exit. Two blocking clusters are different if they differs at least in one pedestrian. That is, if they differ in the number of members or in pedestrians themselves. Fig. 1 shows

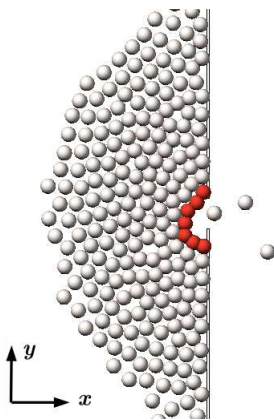


FIG. 1. (Color on-line only) Snapshot of an evacuation process from a $20\text{ m} \times 20\text{ m}$ room, with a single door of 1.2 m width. The blocking structure is identified in red color. The rest of the crowd is represented by white circles. It can be seen three individuals that have already left the room. The desired velocity for the individuals inside the room was $v_d = 6\text{ m/s}$.

(in highlighted color) a *blocking structure* near the door.

We define the *blocking time* as the total time during which the evacuation process is stopped due to any blocking cluster. That is, the sum of the “life time” of each blocking cluster (*blocking delays*).

III. NUMERICAL SIMULATIONS

Most of the simulation processes were performed on a $20\text{ m} \times 20\text{ m}$ room with 225 pedestrians inside. The occupancy density was close to $0.6\text{ individuals/m}^2$ as suggested by healthy indoor environmental regulations [13]. The room had a single exit on one side, as shown in Fig. 1. The door was placed in the middle of the side wall to avoid corner effects.

A few simulation processes were performed on $30\text{ m} \times 30\text{ m}$ and $40\text{ m} \times 40\text{ m}$ rooms with 529 and 961 pedestrians inside, respectively. The door was also placed in the middle of the side wall.

The pedestrians were initially placed in a regular square arrangement along the room with random velocities, resembling a Gaussian distribution with null mean value. The desired velocity v_d was the same for all the individuals. At each time-step, however, the desired direction \mathbf{e}_d was updated, in order to point to the exit.

Two different boundary conditions were examined. The first one included a re-entering mechanism for the outgoing pedestrians. That is, those individuals who were able to leave the room were moved back inside the room and placed at the very back of the bulk with

velocity $v = 0.1\text{ m/s}$, in order to cause a minimal bulk perturbation. This mechanism was carried out in order to keep the crowd size unchanged.

The second boundary condition was the open one. That is, the individuals who left the room were not allowed to enter again. This condition approaches to real situations, and thus, it is useful for comparison purposes.

The simulating process lasted for approximately 2000 s whenever the re-entering mechanism was implemented. If no re-entering was allowed, each evacuation process lasted until 70% of individuals had left the room. If this condition could not be fulfilled, the process was stopped after 1000 s. Whenever the re-entering mechanism was not allowed, at least 30 evacuation processes were run for each desired velocity v_d .

The explored anxiety levels ranged from relaxed situations ($v_d < 2\text{ m/s}$) to extremely stressing ones ($v_d = 20\text{ m/s}$). This upper limit may hardly be reached in real life situations. However, extremely stressing situations may produce similar pushing pressures as those in a larger crowd with moderate anxiety levels (see Ref. [14] for details). Thus, this wide range of desired velocities provided us a full picture of the blocking effects due to high pressures.

The simulations were supported by LAMMPS molecular dynamics simulator with parallel computing capabilities [15]. The time integration algorithm followed the velocity Verlet scheme with a time step of 10^{-4} s . All the necessary parameters were set to the same values as in previous works (see Refs. [5, 14, 16]).

We implemented special modules in C++ for upgrading the LAMMPS capabilities to attain the “social force model” simulations. We also checked over the LAMMPS output with previous computations (see Refs. [5, 16]).

Data recording was done at time intervals of 0.05τ , that is, at intervals as short as 10% of the pedestrian’s relaxation time (see Section II A). The recorded magnitudes were the pedestrian’s positions and velocities for each evacuation process. We also recorded the corresponding social force f_s and granular force f_g actuating on each individual.

IV. RESULTS

A. Evacuation time versus the desired velocity

As a first step we measured the mean evacuation time for a wide range of desired velocities v_d , many of them beyond the interval analyzed by Helbing and co-workers (see Ref. [1]). This is shown in Fig. 2 (filled

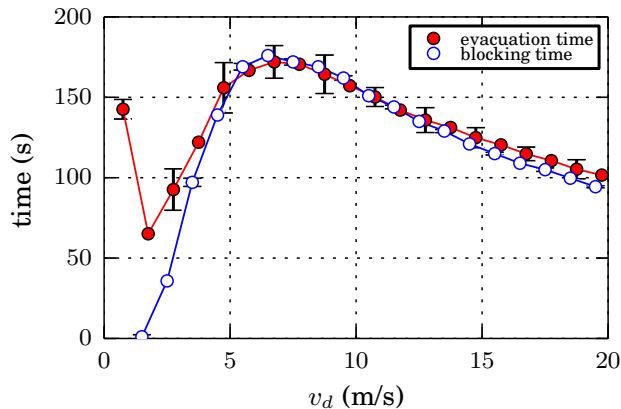


FIG. 2. (Color on-line only) Evacuation time and blocking time as a function of the desired velocity v_d . Both data sets represent the mean values from 60 evacuation processes. The simulated room was 20×20 m with a single door of 1.2 m width on one side. The number of individuals inside the room was 225 (no re-entering mechanism was allowed). The simulation lasted until 160 individuals left the room.

symbols and red line). The *faster is slower* regime can be observed for desired velocities between 2 m/s and 8 m/s (approximately). However, the evacuation time improves beyond this interval, meaning that the greater the pedestrian’s anxiety level, the better with respect to the overall time saving. This phenomenon was reported for both boundary conditions mentioned in Section III.

Therefore, we actually attain a *faster is faster* regime for desired velocities larger than 8 m/s, instead of the expected *faster is slower* regime. This is a novel behavior that has not been reported before (to our knowledge) in the literature. This effect holds even if we include the elastic force introduced by Helbing et al. in Ref. [1] (not shown in Fig. 2).

The overall time performance has been reported to be related to the *clogging delays*, understood as the period of time between two outgoing pedestrians (see Refs. [3–5] for details). But, since most of these time intervals correspond to the presence of *blocking structures* near the door, we examined closely the delays due to blockings for increasing anxiety levels (*i.e.* desired velocities v_d).

Fig. 2 exhibits (in hollow symbols and blue line) the computed blocking time for a wide range of desired velocities. That is, the cumulative “life time” of all the *blocking clusters* occurring during an evacuation process. Notice that the blocking delays become non-vanishing for $v_d > 2$ m/s. This threshold corresponds to those situations where the granular forces become relevant, according to Refs. [3, 4]. It is, indeed, the lower threshold for the *faster is slower* effect.

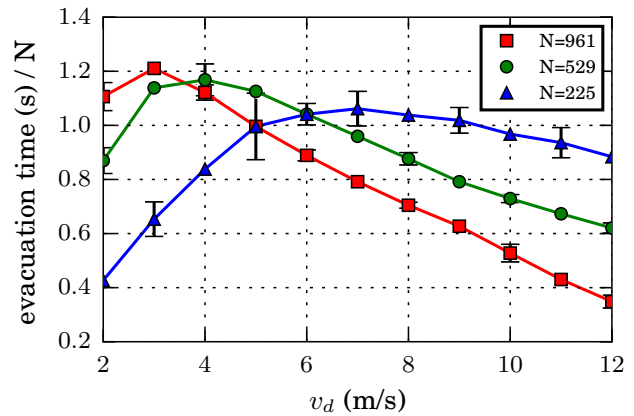


FIG. 3. (Color on-line only) Evacuation time per individual vs. desired velocity for $N=225$, $N=529$ and $N=961$ (no re-entering mechanism was allowed). The room sizes were 20×20 m, 30×30 m and 40×40 m, respectively, with a single door of 1.2 m width on one side. Mean values were computed from 30 evacuation processes until 70% of pedestrians left the room.

No complete matching between the mean evacuation time and the blocking time can be observed along the interval $2 \text{ m/s} < v_d < 4 \text{ m/s}$. This means that the blocking time does not fulfill the evacuation time, but other time waists are supposed to be relevant. We traced back all the time delays experienced by the pedestrian, and noticed that the time lapse between the breakup of the blocking structure and the leaving time of the pedestrians (belonging to this blocking structure) was actually a relevant magnitude. This *transit time* explained the difference between the evacuation time and the blocking time.

According to Fig. 2, the transit time does not play a role for desired velocities larger than $v_d = 4$ m/s. The evacuation time appears to be highly correlated to the blocking delays above this value. Thus, the noticeable enhancement in the evacuation performance taking place between 8 m/s and 20 m/s (*i.e.* the “faster is faster” effect) is somehow related to the enhancement in the blocking time. In other words, the delays associated to the blocking clusters appear to explain the entire *faster is faster* effect.

We next measured the evacuation time for three different crowd sizes. We chose a relatively small crowd (225 pedestrians), a moderate one (529 pedestrians) and a large one (961 pedestrians). The corresponding room sizes were 20×20 m, 30×30 m and 40×40 m, respectively. The results are shown in Fig. 3.

The three situations exhibited in Fig. 3 achieve a *faster is faster* phenomenon, since the slope of each evacuation curve changes sign above a certain desired

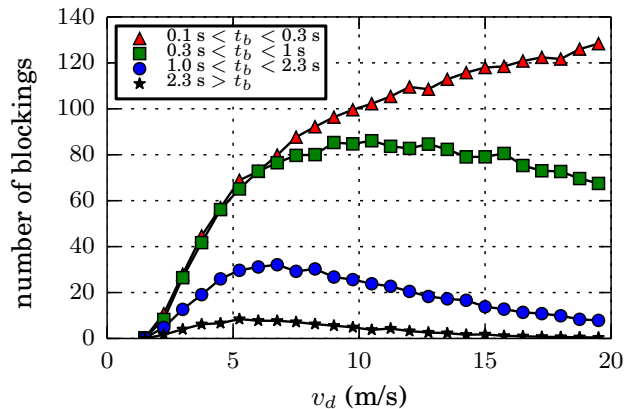


FIG. 4. (Color on-line only) Mean number of blocking delays for four different time intervals (see legend for the corresponding blocking times t_b) as a function of the desired velocity v_d . The simulated room was 20×20 m with a single door of 1.2 m width on one side. The number of individuals inside the room was 225 (no re-entering mechanism was allowed). Mean values were computed from 60 realizations. The simulation lasted until 160 individuals left the room.

velocity. As the number of individuals in the crowd becomes larger, the v_d interval attaining a negative slope increases. That is, only a moderate anxiety level is required to achieve the *faster is faster* phenomenon if the crowd is large enough.

Notice that the larger crowd (*i.e.* 961 individuals) attains the steepest negative slope. Thus, as more people push to get out (for any fixed desired velocity v_d), the faster they will evacuate.

For a better insight of the “faster is faster” phenomenon, we binned the blocking delays into four time intervals or categories. This allowed a quantitative examination of the changes in the delays when moving from the “faster is slower” regime to the “faster is faster” regime. Fig. 4 shows the mean number of blocking delays (for each time interval) as a function of v_d .

The four blocking time intervals represented in Fig. 4 increase for increasing desired velocities until 8 m/s. This is in agreement with the “faster is slower” regime, since the faster the pedestrians try to evacuate, the more time they spend stuck in the blocking structure.

Beyond 8 m/s, the number of blockings corresponding to those time intervals greater than 0.3s reduces (as v_d increases). Thus, the individuals spend less time stuck in the blocking structure for increasing anxiety levels.

It is true that the delays between 0.1s and 0.3s increase for high anxiety levels. But a quick inspection of Fig. 4 shows that this increase (represented in red tri-

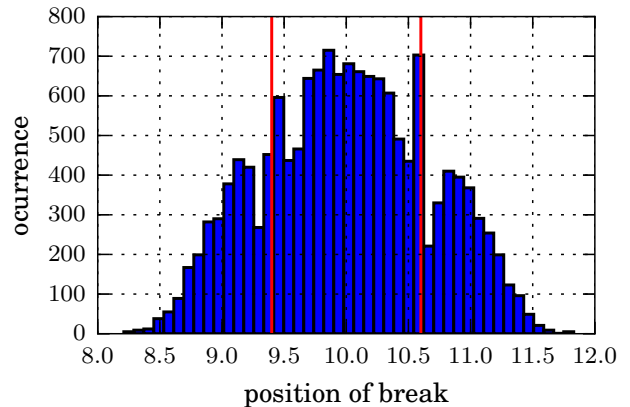


FIG. 5. (Color on-line only) Histogram of the position of the breakup of the blocking cluster. The room size was 20×20 m with 225 pedestrians (no re-entering mechanism was allowed). The door’s width was 1.2 m (from $y = 9.4$ m to $y = 10.6$ m). The vertical red lines represent it’s limits. 30 evacuation processes were performed until 70% of pedestrians left the room. The desired velocity was $v_d = 10$ m/s

angular symbols) is not enough to balance the decrease in the time intervals greater than 0.3s. Consequently, the overall evacuation time follows the same behavior as the long lasting delays (say, the *faster is faster* behavior).

The above research may be summarized as follows. The scenario for high anxiety levels (say, $v_d > 4$ m/s) corresponds to a “nearly always” blocking scenario. However, two different blocking instances can be noticed. The “faster is slower” corresponds to the first instance. The “faster is faster” is the second instance appearing after either high values of v_d or increasing number of pedestrians. Many long lasting blockings seem to break down into shorter blockings, or even disappear (see Fig. 4).

Our results, so far, suggest that the breakup process of the blocking structures needs to be revisited. We hypothesize that a connection between this breakup process and the pedestrian’s pushing efforts should exist. The next two Sections will focus on this issue.

B. Blocking cluster breakup

We now examine the position of the breakups in the blocking cluster. We define the *breakup position* as the one on the y -axis (according to Fig. 1) where any pedestrian gets released from the blocking structure. Fig. 5 exhibits a histogram of the breakup position for a fixed anxiety level ($v_d = 10$ m/s).

The mean value of the distribution in Fig. 5 is close

to $y = 10$ m, that is, the mid-position of the door. This means that the breakups are likely to occur in front of the exit. The same result holds for other desired velocities in the investigated range (not shown). Therefore, this region is of special interest with respect to the breakup process.

From our current simulations and previous work (see Ref. [14]), we realized that the mid-position corresponds to the crowd area of highest pressure (for an exit width of 1.2 m). This is in agreement with the maximum amount of breakups, since higher pushing efforts may help forward the blocking pedestrians.

C. Stationary blocking model

For a better understanding of the relation between the crowd pushing forces and the breakup process, we decided to focus on the behavior of a single pedestrian who tries to get released from the blocking structure.

We mimicked a small piece of the blocking structure (*i.e.* red individuals in Fig. 1) as two individuals standing still, but separated a distance smaller than the pedestrian's diameter. A third pedestrian was set in between the former, mimicking the pedestrian who tries to get released from the blocking structure. Fig. 8a represents this set of three pedestrians. Notice that Fig. 8a may represent any piece of the blocking structure, but according to Section IV B, it will usually correspond to the middle piece of the blocking structure.

The middle pedestrian in Fig. 8a is being pushed from behind by the rest of the crowd. The crowd pushing force f_s points in the x -direction. Two granular forces f_g appear in the opposite direction as a consequence of pedestrian's advancement. More details can be found in Appendix A.

The still pedestrians on both sides experience the repulsion due to the mid-pedestrian, as shown in Fig. 8b. This repulsion f points in the y -direction. We are assuming, however, that the pedestrians on the sides do not move during the breakup process. Thus, the force f should be balanced by the crowd (in the y -direction). This corresponds to the balancing force \mathcal{F} in Fig. 8b. More details can be found in Appendix A.

Notice that our mimicking model assumes that the crowd pushes the mid-pedestrian along the x -direction, while also pushes the still pedestrians along the y -direction. Both forces (f_s and \mathcal{F}) are similar in nature. Actually, for the current geometry, f_s and \mathcal{F} are approximately equal.

The crowd pushing force increases for increasing anx-

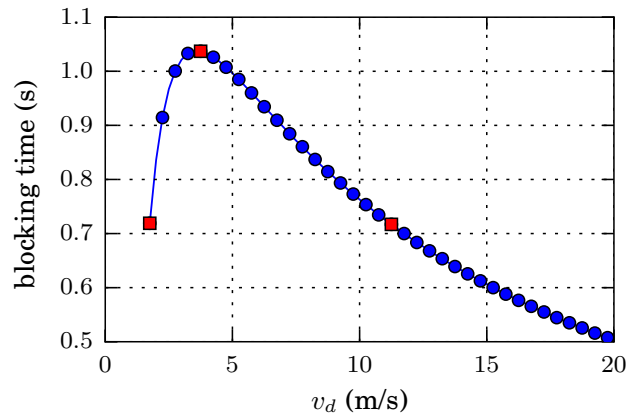


FIG. 6. (Color on-line only) Blocking time of the three pedestrians model (one moving pedestrian between two still ones) as a function of the desired velocity v_d . The initial velocity of the moving pedestrian was set to zero. The crowd pressure was set to $\mathcal{F} = f_s = 2000 v_d$. Each blocking time was recorded when the moving pedestrian lost contact with the other individuals. Desired velocities of $v_d = 1.75$ m/s, $v_d = 3.5$ m/s and $v_d = 11.25$ m/s are indicated in red color (and squared symbols). The blocking time for $v_d = 1.75$ m/s and $v_d = 11.25$ m/s are the same. Only one realization was done for each v_d value.

xiety levels. For a slowly moving crowd, this force varies linearly with v_d , according to Eq. (1). We can therefore set its value as

$$f_s = \mathcal{F} = \beta v_d \quad (6)$$

for any fixed coefficient β . The value of β depends linearly on the number of individuals in the crowd.

We assume a completely blocked situation at the beginning of the simulation. The center of mass of the three pedestrians were initially aligned and the velocity of the individual in the middle was set to zero.

We computed the blocking time on this simple model. This was defined as the period of time required for the moving pedestrian to release from the other two (still ones). This time is supposed to mimic the blocking time of the blocking structure, since the three pedestrians represent a small piece of this structure. Fig. 6 shows the blocking time as a function of the desired velocity v_d .

A comparison between Fig. 2 and Fig. 6 shows the same qualitative behavior for the blocking time, although the scale along the v_d axis is somehow different. The blocking time slope changes sign at 7 m/s in Fig. 2, while Fig. 6 shows a similar change at 3.75 m/s. This discrepancy can be explained because of the chosen value of β .

The chosen value for β in Fig. 6 was 2000 (see caption). This value corresponds to the expected pushing force for a crowd of 225 pedestrians (and $v_d = 2$ m/s). However, as the pedestrians evacuate from the room, the crowd pushing force diminishes. The effective force along the whole process is actually smaller, and so is the β value. Thus, according to Eq. (A7), the “effective” maximum blocking time is expected to lie at a larger v_d value than 3.75 m/s.

The above reasoning is also in agreement with the evacuation time shown in Fig. 3 for an increasing number of pedestrians. The maximum evacuation time takes place at lower anxiety levels (*i.e.* v_d values) as the crowd size becomes larger. Therefore, the pushing force βv_d downscales the *faster is faster* threshold, as expected from our simple model.

So far, the mimicking model for a small piece of the blocking structure exhibits a *faster is slower* instance for low crowd’s pushing forces, and a *faster is faster* instance for large pushing forces. The associated equations for both instances are summarized in Appendix A. This formalism, however, stands for a simple stationary situation. We will release this hypothesis in Section IV D.

D. Non-stationary blocking model

We were able to establish a connection between the breakup process and the crowd pushing forces in Section IV C. Now, we will examine the force balance on the moving pedestrian along the x -axis (see Fig. 8a). As already mentioned, our attention is placed on initially aligned pedestrians with null velocity.

Fig. 7 shows the force balance on the moving pedestrian (of the mimicking model) during the simulated breakup process. The balance is expressed as the ratio between the *positive forces* and the *negative forces*. The former corresponds to the sum of all the forces that push the moving pedestrian towards the exit (*i.e.* the own desired force, and the social force from all the neighbors). The latter corresponds to the force in the opposite direction to the movement (*i.e.* the granular force). According to Section II A and Fig. 8

$$\text{ratio} = \frac{f_s + \mathcal{F} + f_d}{2f_g} \quad (7)$$

where f_s and \mathcal{F} correspond to the pushing forces from the crowd. Both are social forces in nature. Notice, however, that only the contribution on the x -axis is relevant in the mimicking model (see Fig. 8).

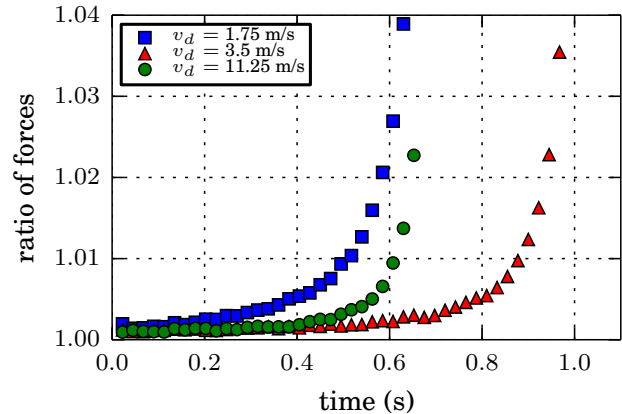


FIG. 7. (Color on-line only) Ratio of *positive forces* (desire force and social repulsion) and *negative force* (granular) on the moving pedestrian as a function of time for three desired velocities (see text for details). The initially velocity of the moving pedestrian was zero. The simulation finished when he loses contact with the other individuals. One realization is done.

Fig. 7 presents three different situations, corresponding to those desired velocities highlighted in red color in Fig. 6. The three situations stand for any *faster is slower* instance, the maximum blocking time instance and any *faster is faster* instance, respectively. But care was taken in choosing similar blocking times for the first and the third situation, in order to achieve a fair comparison.

The three situations shown in Fig. 7 exhibit a ratio close to unity during the first stage of the process. This means that all the forces actuating on the moving pedestrian are approximately balanced. The formalism presented in Appendix A is approximately valid during this stage of the process.

Notice that this quasi-stationary stage lasts until the very end of the breakup process (say, 1% above unity). However, a striking positive slope can be seen during the last stage of each process. The slopes are quite similar on each process (although shifted in time), and thus, this last stage seems not to be relevant in the overall blocking time. We can envisage the last stage as an expelling process before the blocking structure breaks into two pieces.

An important conclusion can be derived from the inspection of Fig. 7: although the breakup process is actually non-stationary, the balance constrain (ratio $\simeq 1$) is quite accurate for the early breakup process.

E. Remarks

From our point of view, the balance constrain (that is, ratio $\simeq 1$) is actually the main reason for the *faster is faster* phenomenon to take place.

Recall that the *positive* forces $f_s + \mathcal{F} + f_d$ correspond to the sum of the pushing forces of the crowd (f_s and \mathcal{F}) and the moving pedestrian's own desire (f_d). The latter, however, is not relevant with respect to the former because most of the pushing effort is done by the crowd (for example, f_d is approximately 10% of f_s for 225 individuals). Thus, the *positive* forces are roughly $f_s + \mathcal{F} = 2\beta v_d$, according to Section IV C and Appendix A 3. The balance constrain becomes approximately

$$\frac{\beta v_d}{f_g} \simeq 1 \quad (8)$$

Eq. (8) is meaningful since it expresses the fact that the *negative* force f_g balances the pushing force, in order to keep the pedestrian moving forward (at an almost constant velocity). However, the granular force is currently $f_g = \kappa v B \ln(\beta v_d/A)$. The $B \ln(\beta v_d/A)$ factor corresponds to the compression between the pedestrian and his (her) neighbor in the blocking structure (see Eq. (A5) for details). Thus

$$v^{-1} \sim \frac{\ln(\beta v_d/A)}{\beta v_d/A} \quad (9)$$

Notice that Eq. (9) resembles the behavior of Fig. 6. The slope of v^{-1} is positive for low anxiety levels (*i.e.* v_d values), but changes sign as the anxiety level becomes increasingly large. Since the blocking time varies as v^{-1} , we may conclude that Eq. (9) mimics the *faster is slower* and the *faster is faster* instances.

The logarithm in Eq. (9) is the key feature for the slope change. Recall from Eq. (A5) that $\ln(\beta v_d/A)$ stands for the compression in the blocking structure. But, although compression increases for increasing pushing forces of the crowd, it seems not enough to diminish the pedestrian velocity in order to hold the *faster is slower* phenomenon at high anxiety levels. Consequently, the blocking time decreases, achieving a *faster is faster* instance.

In Section A 4 a more detailed formalism is exhibited on this issue.

V. CONCLUSIONS

Our investigation focused on the evacuation of extremely anxious pedestrians through a single emergency

door, in the context of the “social force model”. No previous research has been done, to our knowledge, for anxiety levels so high that may cause dangerous pressures (even in relatively small crowds).

Unexpectedly, we found an improvement in the overall evacuation time for desired velocities above 8 m/s (and a crowd size of 225 individuals). That is, the *faster is slower* effect came to an end at this anxiety level, while a novel *faster is faster* phenomenon raised (at least) until a desired velocity of 20 m/s. This unforeseen phenomenon was also achieved for increasingly large crowds and lower desired velocities.

A detailed examination of the pedestrian's blocking clusters showed that the *faster is faster* instance is related to shorter “life times” of the blocking structures near the exit. The long lasting structures taking place at the *faster is slower* instance now breakup into short lasting ones. The breakup is most likely to occur straight in front of the exit.

We mimicked the breakup process of a small piece of the blocking structure through a minimalistic model. The most simple model that we could image was a moving pedestrian between two still individuals. Although its simplicity, it was found to be useful for understanding the connection between the crowd's pushing forces and the blocking breakup process.

The mimicking model for the blocking structure showed that a balance between the crowd's pushing forces and the friction with respect to the neighboring individuals held along the breakup. Only at the very end of the process, the pedestrian was expelled out of the blocking structure.

We concluded from the force balance condition that friction was the key feature for the *faster is faster* instance to take place. As the crowd pushing force increases, the compression between individuals in the blocking structure seems not enough to provide a slowing down in the moving pedestrian. Thus, the *faster is slower* instance switches to a *faster is faster* instance. The latter can be envisaged as brake failure mechanism.

We want to stress the fact that, although we investigated extremely high anxiety situations, *faster is faster* instance may be present at lower desired velocities if the crowd size is large enough. We were able to acknowledge the *faster is faster* phenomenon for desired velocities as low as $v_d = 4$ m/s when the crowd included 1000 individuals approximately.

ACKNOWLEDGMENTS

This work was supported by the National Scientific and Technical Research Council (spanish: Consejo Nacional de Investigaciones Científicas y Técnicas - CONICET, Argentina) grant number PIP 2015-2017 GI, founding D4247(12-22-2016). C.O. Dorso is full researcher of the CONICET. G.A. Frank is assistant researcher of the CONICET. I.M. Sticco and F.E. Cornes have degree in Physics.

Appendix A: A simple blocking model

1. The dynamic

This Appendix examines in detail a very simple model for the time delays in the blocking cluster. We consider a single moving pedestrian stuck in the blocking cluster, as shown in Fig. 8. The moving pedestrian tries to get released from two neighboring individuals that are supposed to remain still during the process. The three pedestrians belong to the same blocking structure, according to the definition given in Section II B. The equation of motion for the pedestrian in the middle of Fig. 8a reads

$$m \frac{dv}{dt} = f_s + f_d - 2f_g \quad (\text{A1})$$

where f_s represents the force due to other pedestrians pushing from behind, f_d represents the moving pedestrian own desire, and f_g represents the corresponding tangential friction due to contact between the neighboring pedestrians. m and v are the mass and velocity of the moving pedestrian (see caption in Fig. 8), respectively. The expressions for f_d and f_g are as follows

$$\begin{cases} f_d = \frac{m}{\tau}(v_d - v) \\ f_g = \kappa(2r - d)v \text{ if } 2r - d > 0 \end{cases} \quad (\text{A2})$$

The granular force f_g expressed in (A2) depends only on the velocity v since the other pedestrians are supposed to remain still. The magnitude $2r - d$ is the difference between the pedestrian's diameter $2r$ and the inter-pedestrian distance d . It represents the compression between two contacting individuals. The other parameters correspond to usual literature values (see Refs. [3, 4]).

The movement equation (A1) expresses the dynamic for the passing through pedestrian. The characteristic time needed for the pedestrian to reach the stationary

state is

$$t_c = \frac{\tau}{1 + \frac{2\kappa\tau}{m}(2r - d)} \quad (\text{A3})$$

and therefore we expect the pedestrian movement to become stationary after this time. It can be easily checked that t_c drops to less than 0.1 s for compression distances as small as 1 mm. This means that the moving pedestrian's velocity will be close to the stationary velocity if the passing through process scales to $t \gg t_c$.

The stationary velocity v_∞ can be obtained from Eq. (A1) and the condition $\dot{v} = 0$. Thus,

$$v_\infty = t_c \left[\frac{f_s}{m} + \frac{v_d}{\tau} \right] \quad (\text{A4})$$

This is (approximately) the velocity that the moving pedestrian will hold most of the time while trying to get released from the other individuals. Thus, the time delay t_d while passing across the still pedestrians will scale as v_∞^{-1} .

Notice from Eqs. (A3) and (A4) that v_∞ decreases for increasing compression values. Also, an increase in the values of f_s or v_d will cause the corresponding increase in v_∞ . The resulting value for v_∞ is a balance between the distance $2r - d$ and the forces f_s or v_d . The distance $2r - d$, however, resembles the compression between members of the same blocking cluster, while the force f_s corresponds to individuals out of the blocking cluster.

2. The force balance

Fig. 8b shows a schematic diagram for the forces applied to one of the still individuals. The force f in Fig. 8b represents the repulsive feeling actuating on the still individual due to the moving pedestrian. The force \mathcal{F} is the required counter force necessary to keep the individual still. That is, \mathcal{F} balances the repulsive feeling f for a specific compression distance $2r - d$ (and fix values of f_s and v_d). According to Section II A, the relationship between the compression distance and \mathcal{F} (or f) is as follows

$$2r - d = B \ln(\mathcal{F}/A) \quad (\text{A5})$$

for the known values A and B .

The relation (A5) can be applied to the expression (A3) for computing the characteristic time t_c . This means that t_c may be controlled by \mathcal{F} , and consequently, it controls the stationary velocity v_∞ , according to

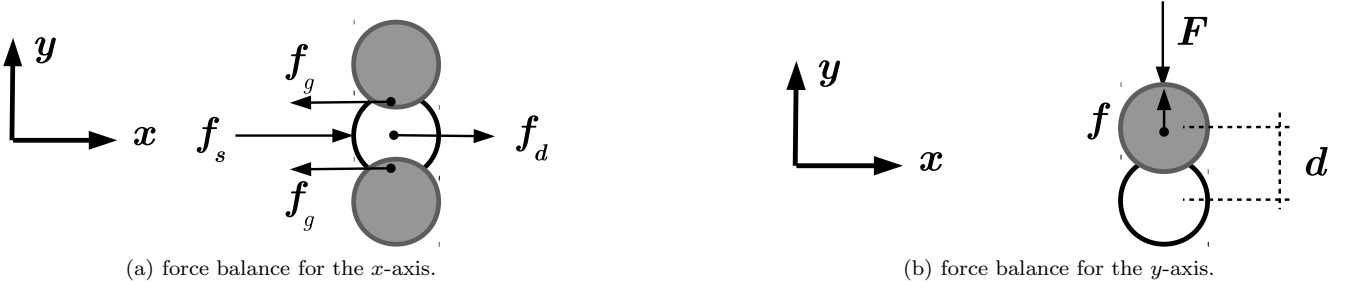


FIG. 8. Force balance for a moving pedestrian between two still individuals. The moving pedestrian is represented by the white circle, while the gray circles correspond to the still individuals. The movement is in the $+x$ direction. f_s represents the (mean) force due to other pedestrians pushing from behind. f_d is the moving pedestrian's own desire. f_g corresponds to the tangential friction (*i.e.* granular force) between the moving pedestrian and his (her) neighbors. \mathcal{F} and f are the forces acting on the upper (still) pedestrian. f corresponds to the social repulsive force due to the moving pedestrian, while \mathcal{F} represents the counter force for keeping the pedestrian still.

(A4). Actually, the value of v_∞ results from the balance between \mathcal{F} and f_s (and v_d).

3. The crowd context

The above relations for a single moving pedestrian sliding between two still individuals should be put in the context of an evacuation process. These three pedestrians may belong to a “blocking structure”, as defined in Section II B. The blocking structure may be surrounded by a large number of pedestrians that do not belong to this structure, but continuously pushes the structure towards the exit. Therefore, the forces f_s and \mathcal{F} are similar in nature and somehow represent the pressure acting on the blocking structure from the surrounding crowd.

The pressure from the crowd depends on the anxiety level of the pedestrians. It has been shown that, at equilibrium, the crowd pressure grows linearly with the desired velocity v_d and the number of individuals pushing from behind (see Ref. [14]). It seems reasonable, as a first approach, that f_s and \mathcal{F} varies as βv_d for any fixed coefficient β .

The forces f_s and \mathcal{F} may be replaced by βv_d in Eq. (A4) for the evacuation process scenario, as explained in Section IV C. Thus, the stationary velocity v_∞ only depends on the desired velocity of the pedestrians (and the total number of individuals). Fig. 9 shows the behavior of the time delay (v_∞^{-1}) for a wide range of desired velocities v_d .

The continuous line in Fig. 9 exhibits a local minimum and a maximum at $v_d = 1$ m/s and $v_d = 3.7$ m/s, respectively. The behavioral pattern for $v_d < 1$ m/s corresponds to non-contacting situations (that is,

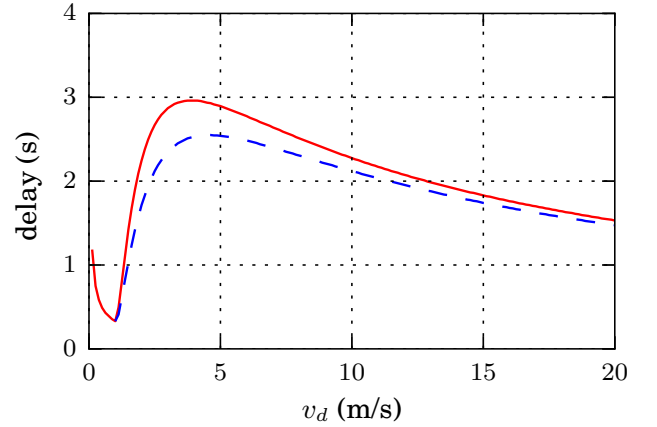


FIG. 9. (Color on-line only) Time delay (v_∞^{-1}) for a moving individual passing between two still pedestrians, as shown in Fig. 8. The time interval was measured along 10 m across the still pedestrians. The initial velocity was v_d . The continuous line corresponds to the measured delay for $\beta v_d = 2000 v_d$ and $f = A \exp[(2r - d)/B]$ (see text for details). The dashed line corresponds to the measured delay for $\beta v_d = 2000 v_d$ and $f = A \exp[(2r - d)/B] + k(2r - d)$ (see text for details). The minimum time delay for both lines takes place at $v_d = 1$ m/s. The maximum time delay for the continuous line takes place at $v_d = 3.7$ m/s, while for the dashed line takes place at $v_d = 4.2$ m/s.

$2r - d < 0$). The characteristic time for this regime is $t_c = \tau$, and thus, the time delay decreases for increasing values of v_d , according to Eq. (A4).

The regime for $v_d > 1$ m/s corresponds to those situations where the moving pedestrian gets in contact with the two still individuals. Since the compression distance $2r - d$ becomes positive, there is a reduction in the characteristic time t_c , according to Eq. (A3). This reduction actually changes the value of the stationary velocity v_∞ ,

as expressed in (A4). It is not immediate whether the t_c reduction increases or decreases the velocity v_∞ . A closer inspection of the v_∞ behavioral pattern is required.

The computation of the slope for v_∞ with respect to v_d gives the following expression

$$\frac{dv_\infty}{dv_d} = \left[1 - \frac{2\kappa B}{m} t_c \right] \frac{v_\infty}{v_d} \quad (\text{A6})$$

This expression shows a change of sign in the slope of v_∞ for increasing values of v_d . It can be checked over that the expression enclosed in brackets is negative for small compressions, but as t_c decreases (due to v_d increments), it becomes positive. The vanishing condition for (A6) is

$$B \ln \left(\frac{\beta v_d}{A} \right) = B - \frac{m}{2\kappa\tau} \quad (\text{A7})$$

The last term on the right becomes neglectable with respect to B for the current literature values. Thus, the maximum time delay (v_∞^{-1}) takes place close to $v_d = 2.7 A/\beta$. The corresponding compression distance for this desired velocity is $2r - d = B$.

4. Remarks

The above computations show two relevant v_d values: the one where a minimum time delay takes place and the one where the maximum time delay happens. The former corresponds to $v_d = A/\beta$, or equivalently, $2r - d = 0$. The latter corresponds to $v_d = 2.7 A/\beta$ or $2r - d = B$ (approximately).

The forces f_s and \mathcal{F} are similar in nature for the evacuation scenario. Therefore, \mathcal{F} can be replaced by f_s in the Eq. (A5) for the stationary passing through process shown in Fig. 8. The stationary balance for Eq. (A1) then reads

$$A e^{(2r-d)/B} + \frac{mv_d}{\tau} = \left[2\kappa(2r-d) + \frac{m}{\tau} \right] v_\infty \quad (\text{A8})$$

Accordingly, the time delay reads

$$v_\infty^{-1} = \frac{1 + \frac{2\kappa\tau}{m}(2r-d)}{\frac{A\tau}{m} e^{(2r-d)/B} + v_d} \quad (\text{A9})$$

Notice from this expression that small increments of $2r - d$ produce increasing values of the time delay v_∞^{-1} if $2r - d < B$. But, further compression increments (that is, increments beyond $2r - d > B$) reduce the time delay,

since the exponential function grows increasingly fast.

The above observations give a better understanding for the local maximum exhibited in Fig. 9. The positive slope range for v_∞^{-1} corresponds to small values of f_s (that is, small values for the exponential function in (A9)), while the negative slope range (beyond the local maximum) corresponds to high f_s values.

Although Fig. 9 is in correspondence with Eq. (A6), the local maximum does not actually take place at $v_d = 2.7 \text{ m/s}$ but at $v_d = 3.7 \text{ m/s}$. This is right since Fig. 9 represents a complete simulation of the moving pedestrian instead of the stationary model for the pedestrian at the crossing point between the still individuals, as expressed in Eq. (A1) and shown in Fig. 8.

Fig. 9 also shows in dashed line the time delay for individuals with non-neglectable elastic compressions (see caption for details). The local maximum also appears but for lower time delay values.

-
- [1] D. Helbing, I. Farkas, and T. Vicsek, *Nature* **407**, 487 (2000).
- [2] J. M. Pastor, A. Garcimartín, P. A. Gago, J. P. Peralta, C. Martín-Gómez, L. M. Ferrer, D. Maza, D. R. Parisi, L. A. Pugnaloni, and I. Zuriguel, *Phys. Rev. E* **92**, 062817 (2015).
- [3] D. Parisi and C. O. Dorso, *Physica A* **354**, 606 (2005).
- [4] D. Parisi and C. O. Dorso, *Physica A* **385**, 343 (2007).
- [5] G. Frank and C. O. Dorso, *Physica A* **390**, 2135 (2011).
- [6] F. Cornes, G. Frank, and C. Dorso, *Physica A: Statistical Mechanics and its Applications* **484**, 282 (2017).
- [7] A. Janda, I. Zuriguel, A. Garcimartín, L. A. Pugnaloni, and D. Maza, *EPL (Europhysics Letters)* **84**, 44002 (2008).
- [8] A. Garcimartín, I. Zuriguel, L. A. Pugnaloni, and A. Janda, *Phys. Rev. E* **82**, 031306 (2010).
- [9] C. Lozano, G. Lumay, I. Zuriguel, R. C. Hidalgo, and A. Garcimartín, *Phys. Rev. Lett.* **109**, 068001 (2012).
- [10] C. Lozano, A. Janda, A. Garcimartín, D. Maza, and I. Zuriguel, *Phys. Rev. E* **86**, 031306 (2012).
- [11] K. Suzuno, A. Tomoeda, and D. Ueyama, *Phys. Rev. E* **88**, 052813 (2013).
- [12] J. Stokes, *NASA-MSFC* **2.5**, 5 (1976).
- [13] M. Mysen, S. Berntsen, P. Nafstad, and P. G. Schild, *Energy and Buildings* **37**, 1234 (2005).
- [14] I. Sticco, G. Frank, S. Cerrotta, and C. Dorso, *Physica A: Statistical Mechanics and its Applications* **474**, 172 (2015).
- [15] S. Plimpton, *Journal of Computational Physics* **117**, 1 (1995).
- [16] G. Frank and C. O. Dorso, *International Journal of Modern Physics C* **26**, 1 (2015).